CONTINUED DEVELOPMENT OF A CLOUD DROPLET FORMATION PARAMETERIZATION FOR GLOBAL CLIMATE MODELS

A Thesis
Presented to
The Academic Faculty

By

Christos Fountoukis

In Partial Fulfillment
Of the Requirements for the Degree
Master of Science in Chemical Engineering

Georgia Institute of Technology

August 2005

CONTINUED DEVELOPMENT OF A CLOUD DROPLET FORMATION PARAMETERIZATION FOR GLOBAL CLIMATE MODELS

Approved by:

Dr. Athanasios Nenes, ChBE
Georgia Institute of Technology

Dr. Amyn Teja, ChBE
Georgia Institute of Technology

Dr. Yuhang Wang, EAS
Georgia Institute of Technology

Date Approved: 29/06/2005

In memory of my grandfather, Christos,
To my family, for their priceless support,
and to all those who inspired me during this journey…

ACKNOWLEDGMENT

I would like to thank my advisor, Dr. Athanasios Nenes, for providing me with his time, expert guidance and valuable support.

This research was supported by a NASA EOS-IDS, a NASA New Investigator Award, and by Georgia Institute of Technology faculty startup funds.

TABLE OF CONTENTS

Acknowledgments iv

List of Tables vii

List of Figures viii

List of Symbols or Abbreviations x

Summary xii

Chapter 1 Introduction 1

Chapter 2 Development of an Aerosol Activation Parameterization for Lognormal Aerosol 7

2.1 Introduction: the Nenes and Seinfeld (2003) Parameterization 7

2.2 Representation of the CCN Spectrum 8

2.3 Calculating s_{max} and Droplet Number Concentration 10

2.4 Calculation of Integral $I(0,s_{max})$ 11

2.5 Using the Parameterization 13

Chapter 3 Including Size-dependant Growth Kinetics into NS 16

3.1 Introduction 16

3.2 Implementing Size-dependant D_v into NS 17

3.3 Determination of $D_{p,big}$ and $D_{p,low}$ 19

Chapter 4 Evaluation of Modified NS Parameterization 25

4.1 Method 25

4.2 Evaluation of the Modal Formulation 27

4.3 Evaluation of Parameterization with Modified Water Vapor Mass Transfer 31

Chapter 5 Conclusions 35

Appendix A: Simulations used for deriving the optimal $D_{p,big}$ and $D_{p,low}$ used for calculating $D_{v,ave}$ 37

References 43

LIST OF TABLES

Table 1	Simulations considered for empirically determining $D_{p,big}$ and $D_{p,low}$ of $D_{v,ave}$	20
Table 2	Simulation data for the optimization process of $D_{p,big}$ and $D_{p,low}$ (α_c=0.001)	40
Table 3	Simulation data for the optimization process of $D_{p,big}$ and $D_{p,low}$ (α_c=0.005)	41
Table 4	Simulation data for the optimization process of $D_{p,big}$ and $D_{p,low}$ (α_c=0.042)	42
Table 5	Aerosol and updraft velocity conditions considered in the parameterization evaluation	26
Table 6	Aerosol characteristics for the multimodal simulations of Table 2. Distributions taken from Whitby (1978). $D_{g,i}$ is in μm; N_i is in cm^{-3}	27
Table 7	Size distribution parameters of single mode (SM) and tri-modal (TM) test cases shown in figure 8	37

LIST OF FIGURES

Figure 1	Parameterization algorithm (lognormal formulation)	15
Figure 2	Droplet number concentration as predicted by the modified NS parameterization and by the cloud parcel model, using the sectional formulation. Results for both theoretical and empirical $D_{v,ave}$ are presented. The other simulation characteristics are given in the text	24
Figure 3	Droplet number concentration as predicted by the modified NS parameterization using the sectional and the modal formulations. Cases considered were for a single mode lognormal aerosol with $D_{p,g}$ ranging between 0.05 to 0.75μm, σ_i ranging between 1.1 to 2.5, updraft conditions ranging between V = 0.1 to 3.0 ms^{-1} and for chemical composition of pure $(NH_4)_2SO_4$, pure NaCl, and 50% $(NH_4)_2SO_4$ - 50% insoluble. Ambient P and T were set to 800 mbar and 283 K, respectively. The sectional formulation used 200 sections for discretizing the lognormal distribution. Results are for four values of a_c	28
Figure 4	Droplet number concentration as predicted by the NS parameterization and by the cloud parcel model for all the aerosol size distributions and updraft velocities of Table 2. All simulations assume perfect water vapor accommodation (a_c = 1.0), P = 800mbar and T = 283K	29
Figure 5	Droplet number concentration as predicted by the NS parameterization and by the cloud parcel model for cases SM1, SM2 and SM3 of Table 2, and for a_c = 1.0, a_c = 0.01, and a_c = 0.005. All simulations assume P = 800mbar and T = 283K	30
Figure 6	Droplet number concentration as predicted by the modified NS parameterization and by the cloud parcel model for cases SM3 and SM4 of Table 5, and for a_c = 0.042. All simulations assume P = 800mbar and T = 283K	33

Figure 7 Droplet number concentration as predicted by the modified NS parameterization and by the cloud parcel model for case TM of Table 5, and for $a_c = 0.005$. All simulations assume P = 800mbar and $T = 283$K 34

Figure 8 Droplet number concentration as predicted by the modified NS parameterization and by the cloud parcel model for all cases considered in Table 7. All simulations assume P = 800mbar and $T = 283$K 38

LIST OF SYMBOLS or ABBREVIATIONS

c_p	Heat capacity of air
D_c	Critical Diameter
$D_{g,i}$	Geometric mean diameter of mode i
D_p	Particle diameter
$D_{p,big}$	Upper particle size bound
$D_{p,low}$	Lower particle size bound
$D_{p(\tau)}$	Size of a CCN when $s=s_c$
D_v	Diffusivity of water vapor in air
D_v'	Corrected diffusivity of water vapor in air
$F^s(s)$	CCN spectrum
k_a'	Thermal conductivity of air
L	Latent heat of condensation of water
M_s	Solute molecular weight
M_w	Molecular weight of water
N_d	Activated droplet number
N_i	Aerosol number concentration of mode i
$n^d(D_p)$	Size distribution
n_m	Number of modes in the distribution
$n^s(s)$	Supersaturation distribution
p	Ambient pressure
p^s	Water vapor pressure

p_v^*	Saturation vapor pressure of water
R	Universal gas constant
s	Supersaturation
s_c	Critical supersaturation
$s_{g,i}$	Critical supersaturation of particle with diameter $D_{g,i}$
s_{max}	maximum parcel supersaturation
s_{part}	Partitioning critical supersaturation
T	Parcel temperature
t_{max}	Time of maximum supersaturation
V	Cloud parcel updraft velocity

Greek letters

a_c	Mass accommodation (or condensation) coefficient
Δ	Descriminant
v	Effective Van't Hoff factor
ρ_s	Density of the solute
ρ_w	Density of water
σ	Droplet surface tension
σ_i	Geometric standard deviation or mode i
τ	Time needed for activation

SUMMARY

This study presents continued development of the Nenes and Seinfeld (2003) cloud droplet activation parameterization. First, we expanded the formulation to *i)* allow for a lognormal representation of aerosol size distribution, and, *ii)* include a size-dependant mass transfer coefficient for the growth of water droplets to accommodate the effect of size (and potentially organic films) on the droplet growth rate. The performance of the new scheme is evaluated by comparing the parameterized cloud droplet number concentration with that of a detailed numerical activation cloud parcel model. The resulting modified parameterization robustly and closely tracks the parcel model simulations, even for low values of the accommodation coefficient (average error 4.1±1.3%). The modifications to include the effect of accommodation coefficient do not increase the computational cost but substantially improves the parameterization performance. This work offers a robust, computationally efficient and first-principles approach for directly linking complex chemical effects (e.g., surface tension depression, changes in water vapor accommodation, solute contribution from partial solubility) on aerosol activation within a global climate modeling framework.

CHAPTER 1

INTRODUCTION

At steady state, the Earth's energy balance requires that the flux of incoming energy from the sun, most of which is in the visible part of the spectrum, must be balanced by an equal outgoing flux of infrared radiation. Any deviation on either side of this balance, incoming or outgoing, drives the earth's climate to a new warmer or cooler equilibrium state so that the requirement for energy balance will again be satisfied. Greenhouse gases intercept some of the outgoing longwave radiation and thereby act to force the earth's surface to come to a higher equilibrium temperature.

In contrast to greenhouse gases, which interact with infrared radiation, atmospheric particulate matter, or "aerosols" can influence both sides of the energy balance. They reflect a significant amount of radiation back to space, thus enhancing the planetary albedo (also known as the aerosol "direct" radiative effect). By acting as cloud condensation nuclei (CCN), they also have a strong impact on cloud optical properties, the latter of which play a profound role on climate. For a given liquid water content, an increase in the number concentration of aerosol particles, which results in an increase of CCN, will lead to larger droplet concentrations; this means the cloud will have droplets with smaller effective radius, thus increasing the cloud shortwave reflectivity (also known as the "1_{st} aerosol indirect radiative effect"). The decrease in droplet size also may decrease the precipitation efficiency of clouds, thus producing longer-lived clouds (this is known as the "2_{nd} aerosol indirect radiative effect"). Most of the observed uncertainty in

radiative forcing is caused by the aerosol indirect effect since it involves microphysical properties that are not well understood, or easily parameterized. The resulting radiative forcing enhances the cooling of the atmosphere as opposed to the greenhouse effect, hence making the net global mean anthropogenic forcing estimates range from positive to negative. Therefore, reducing the uncertainty of indirect forcing by anthropogenic aerosols is, nowadays, highly anticipated (IPCC, 2001).

Calculation of cloud properties from precursor aerosol in general circulation models (GCMs) has often relied on empirical (phenomenological) correlations (e.g. Boucher and Lohmann, 1995; Gultepe and Isaac, 1996), which are subject to significant uncertainty. To address this limitation, first-principle approaches (e.g., Ghan *et al*., 1997; Lohmann *et al*., 1999) have been proposed, which require setting up a cloud droplet number balance in each GCM grid cell; processes such as the activation of aerosol into cloud droplets, evaporation, and collision/coalescence affect droplet number concentration. Explicitly resolving each of these processes is far beyond anything computationally feasible for GCMs, so, a prognostic GCM estimate of the aerosol indirect effect must rely on parameterizations of aerosol-cloud interactions.

The chemical complexity and heterogeneity of global aerosols can have an important effect on activation and must be included in aerosol-cloud interaction studies (e.g., Nenes *et al*., 2001; Rissman *et al*., 2002; Lance *et al*., 2004). Incorporating such complexity into extant parameterizations is not a trivial task. For example, the presence of surface active species may facilitate the activation of cloud condensation nuclei (CCN) into cloud droplets (Facchini *et al*., 1999). The influence of surfactants depends on their concentration (e.g., Shulman *et al*., 1996; Charlson *et al*., 2001) which varies

considerably with CCN dry size (e.g., Charlson *et al*., 2001; Rissman *et al.*, 2004). Because of this, an explicit relationship between the critical supersaturation, s_c (the supersaturation required to activate a CCN into cloud droplet) and the critical diameter, D_c is not possible (Li *et al*., 1998; Rissman *et al*., 2004), and becomes challenging to incorporate into mechanistic parameterizations (Rissman *et al*., 2004). Furthermore, the droplet growth rate may be influenced by the presence of organic films (Feingold and Chuang, 2002; Chuang, 2003; Nenes *et al*., 2002; Medina and Nenes, 2004; Lance *et al.*, 2004) and slightly soluble substances (Shantz *et al.*, 2003; Shulman *et al.,* 1996) both of which could have an impact on cloud droplet number (Nenes *et al.*, 2002).

Considering a droplet of diameter D_p containing n_w moles of water and n_s moles of solute (e.g. nonvolatile salt), the relation between the water vapor pressure over the droplet solution of diameter D_p, $p_w(D_p)$, and the water vapor pressure over a flat surface, p^o, is given by the equation (Seinfeld and Pandis, 1998):

$$\ln\left(\frac{p_w(D_p)}{p^o}\right) = \frac{4M_w\sigma_w}{RT\rho_w D_p} - \frac{6n_s M_w}{\pi\rho_w D_p^3}$$

The above equation describes the Kohler theory, expressing the two effects that determine the vapor pressure over an aqueous solution droplet-the Kelvin effect that tends to increase vapor pressure and the solute effect that tends to decrease vapor pressure. The ratio p_w/p^o is the saturation ratio required for droplet equilibrium. If the environment reaches a saturation larger than the critical saturation of a particle, S_c, then, according to Kohler theory, the particle is considered to be activated and starts growing rapidly, becoming a cloud droplet.

Chemical effects on droplet growth, such as those mentioned earlier in this chapter, are not considered in the Köhler theory described above. The effect of partially soluble

materials is to increase the solute effect. Physically, partial solubility lowers the vapor pressure of CCN facilitating their ability to activate. Furthermore, the presence of organics that decrease the surface tension of droplets, makes the Kelvin effect of Kohler equation less significant, thus facilitating the activation process.

The ability of a given particle to become activated depends on its size and chemical composition and on the maximum supersaturation experienced by the particle. If, for example, the ambient relative humidity (RH) does not exceed 100%, no particle will be activated and a cloud cannot be formed. This RH increase is usually the result of cooling of a moist air parcel. If an air parcel ascends in the atmosphere, its pressure decreases, the parcel expands, and its temperature drops. The simplest model of such a process assumes that during this expansion there is no heat exchanged between the rising parcel of air and the environment (adiabatic cooling). Although numerical models with a detailed treatment of cloud droplet activation have existed for many years, the computational burden associated with such simulations largely prohibits their use in global models. Therefore, treatment of aerosol-cloud interactions must rely on parameterizations.

Previous researchers have undertaken a variety of diagnostic parameterizations to derive the empirical relationships between the cloud droplet number concentration and aerosol number concentration (Boucher and Lohmann, 1995; Gultepe and Isaac, 1996). Diagnostic parameterizations yield a wide range in the estimates of the global annual average indirect aerosol forcing, emphasizing for more robust, physically-based modeling approaches. Prognostic, physically-based parameterizations have emerged within the last decade.

One of the most comprehensive parameterizations developed to date is by Nenes and Seinfeld (2003) (hereafter referred to as "NS"). NS can treat internally or externally mixed aerosol with size-varying composition and can include the depression of surface tension from the presence of surfactants, insoluble species and slightly soluble species within a framework in which minimal amount of empirical information is used (e.g., of all 200 cases tested by NS, only 20% required a correlation derived from a numerical parcel model). Despite the significant improvement in droplet number prediction compared to other parameterizations, NS may underestimate the droplet number concentration, and cannot, as most other mechanistic parameterizations, explicitly consider the potential delays in droplet growth from the presence of film forming compounds. Furthermore, NS employs a sectional representation of aerosol size, which may impose an unnecessary computational burden for global climate models using lognormal aerosol size distributions. These shortcomings are addressed in this study.

The research presented here extends the NS parameterization by i) providing a formulation of the parameterization for a lognormal description of the aerosol size distribution, and, ii) including explicit size-dependence of water vapor diffusivity. The latter overcomes the underprediction tendency of the original formulation, and, allows to explicitly include the effect of organics that may affect the condensational growth of CCN.

Chapter 1 serves as an introduction to the theory of aerosol – cloud interactions and presents the motivation of this work. Chapter 2 describes the formulation for lognormal aerosol of the NS parameterization giving a brief description of the original parameterization. Chapter 3 deals with the problem of the potential delays in droplet

growth from the presence of film forming compounds. Chapter 4 presents an evaluation of the modified NS parameterization and, finally, Chapter 5 discusses the overall results.

CHAPTER 2

DEVELOPMENT OF AN AEROSOL ACTIVATION PARAMETERIZATION FOR LOGNORMAL AEROSOL

This chapter develops an aerosol activation parameterization based on the work of Nenes and Seinfeld (2003). The new formulation is most appropriate for a lognormal description of the aerosol size distribution, which is used in many of the global climate models in use today.

2.1 Introduction: the Nenes and Seinfeld (2003) parameterization

NS is based on a generalized sectional representation of aerosol size and composition (internally or externally mixed), with size-varying composition. The NS methodology involves two steps: The first involves the representation of the aerosol number and the chemical composition distribution with respect to size and the calculation of the number concentration of droplets that can potentially form at a certain level of supersaturation (the "CCN spectrum") using the appropriate form of Köhler theory (e.g., Seinfeld and Pandis, 1998). The modified Kohler theory used, embodies the effects of surfactants and slightly soluble species to compute the supersaturation needed for a CCN to activate. In the second step, the CCN spectrum is included within the dynamical framework of an adiabatic parcel with a constant updraft velocity (or cooling rate), to compute the maximum supersaturation, s_{max}, achieved during the cloud parcel ascent. Calculation of

s_{max} is based on a balance between water vapor availability from cooling and water vapor depletion from the condensational growth of the CCN. CCN with $s_c \leq s_{max}$ will then be activated into droplets.

NS introduce the concept of "population splitting" to obtain an analytical expression for the water vapor condensation rate; an integro-differential equation is this way reduced to an algebraic equation which can be numerically solved. Population splitting entails division of the CCN into two separate populations: those which have a size close to their critical diameter (the diameter a CCN must grow to before experiencing unstable growth), and those that do not. As a result of this approach, kinetic limitations on droplet growth are explicitly considered. A common assumption made in other parameterizations is that the CCN grows instantaneously to its critical diameter when the parcel supersaturation becomes equal to the CCN's critical supersaturation; that is the activation process is not kinetically limited. When this condition is not satisfied, it can be a source of significant error in the prediction of the number of activated droplets (Nenes *et al*., 2001). In NS, compared with other mechanistic parameterizations, the reliance on empirical information or correlations is significantly reduced.

2.2 Representation of the CCN spectrum

Using the nomenclature of Nenes and Seinfeld (2003), size distributions, $n^d(D_p)$, are taken to be of the single or multiple lognormal form,

$$n^d(D_p) = \frac{dN}{d\ln D_p} = \sum_{i=1}^{n_m} \frac{N_i}{\sqrt{2\pi}\ln\sigma_i} \exp\left[-\frac{\ln^2(D_p / D_{g,i})}{2\ln^2\sigma_i}\right] \qquad (1)$$

where D_p is particle diameter, N_i is the aerosol number concentration, $D_{g,i}$ is the geometric mean diameter of mode i, σ_i is the geometric standard deviation for mode i, and n_m is the number of modes in the distribution.

If the chemical composition of an aerosol mode does not vary with size, then $n^d(D_p)$ can be mapped to supersaturation space and the critical supersaturation distribution, $n^s(s)$, can be obtained as follows:

$$n^s(s) = \frac{dN}{ds} = -\frac{dN}{d\ln D_p} \cdot \frac{d\ln D_p}{ds} \tag{2}$$

where

$$\frac{dN}{d\ln D_p} = \sum_{i=1}^{n_m} \frac{N_i}{\sqrt{2\pi}\ln\sigma_i} \exp\left[-\frac{\ln^2(D_p/D_{g,i})}{2\ln^2\sigma_i}\right] \tag{3}$$

The critical supersaturation of a particle with diameter D_p is

$$s = \frac{2}{\sqrt{B}} \cdot \left(\frac{A}{3D_p}\right)^{3/2} \tag{4}$$

where $A = \frac{4\sigma M_w}{\rho_w}$ and $B = \frac{\nu\rho_s M_w}{\rho_w M_s}$ (Seinfeld and Pandis, 1998), ρ_s is the solute density, M_s the solute molecular weight, ν is the number of ions resulting from the dissociation of one solute molecule. From Equation (4) we obtain,

$$\frac{d\ln D_p}{ds} = -\frac{2}{3s} \tag{5}$$

and

$$\frac{D_p}{D_g} = \left(\frac{s_g}{s}\right)^{2/3} \tag{6}$$

Substitution of Equations (1), (3), (5) and (6) into (2) yields the critical supersaturation distribution,

$$n^s(s) = \sum_{i=1}^{n_m} \frac{2N_i}{3s\sqrt{2\pi}\ln\sigma_i} \exp\left[-\frac{\ln^2(s_{g,i}/s)^{2/3}}{2\ln^2\sigma_i}\right] \tag{7}$$

where $s_{g,i}$ is the critical supersaturation of a particle with diameter $D_{g,i}$.

From Equation (7), the CCN spectrum (concentration of particles with $s_c \le s$), $F^s(s)$, is given by

$$F^s(s) = \int_0^s n^s(s)ds = \sum_{i=1}^{n_m} \frac{N_i}{2} erfc\left[\frac{2\ln(s_{g,i}/s)}{3\sqrt{2}\ln\sigma_i}\right] \tag{8}$$

If the maximum parcel supersaturation, s_{max}, is known, the activated droplet number, N_d, can be calculated from Equation (8), as

$$N_d = F^s(s_{\max}) \tag{9}$$

2.3 Calculating s_{max} and droplet number concentration

The maximum supersaturation, s_{max}, is calculated from an equation that expresses the water vapor balance (Nenes and Seinfeld, 2003):

$$\frac{2aV}{\pi\gamma\rho_w} - Gs_{\max}I(0, s_{\max}) = 0 \tag{10}$$

where,

$$a = \frac{gM_wL}{c_pRT^2} - \frac{gM_a}{RT}, \qquad \gamma = \frac{pM_a}{p^sM_w} + \frac{M_wL^2}{c_pRT^2} \tag{11}$$

and V is the cloud parcel updraft velocity, ρ_w is the density of water, T is the parcel temperature, M_w is the molecular weight of water, L is the latent heat of condensation of

water, p^s is the water vapor pressure, c_p is the heat capacity of air, p is the ambient pressure and R is the universal gas constant. G in Equation (10) is given by

$$G = \frac{1}{\frac{\rho_w RT}{p_v^* D_v^{'} M_w} + \frac{L\rho_w[(LM_w / RT) - 1]}{k_a^{'} T}} \tag{12}$$

where p_v^* is the saturation vapor pressure of water, $D_v^{'}$ is the diffusivity of water vapor in air and $k_a^{'}$ is the thermal conductivity of air.

The quantity $I(0,s_{max})$ in Equation (10) is defined as,

$$I(0, s_{\max}) = \int_0^{S_{\max}} [D_p^2(\tau) + \frac{G}{aV}(s_{\max}^2 - s(\tau)^2)]^{1/2} n(s) ds \tag{13}$$

$D_p(\tau)$ denotes the size of a CCN when it is exposed to $s = s_c$; τ is the time needed (above cloud base) to develop the supersaturation needed for its activation. A common assumption (e.g., used by *Ghan et al*., 1993) is that CCN instantaneously activate, i.e., $D_p(\tau)$ is equal to the CCN critical diameter, $D_c = 8M_w\sigma/3RT\rho_w s$, (where σ is the droplet surface tension at the point of activation). Evaluation of $I(0,s_{max})$ and substitution into Equation (10) results in an algebraic equation that can be solved for s_{max}.

2.4 Calculation of Integral $I(0,s_{max})$

We can approximate $I(0,s_{max})$ by employing the "population splitting" concept of NS:

$$I(0, s_{\max}) = I_1(0, s_{part}) + I_2(s_{part}, s_{\max}) \tag{14}$$

where s_{part} is the "partitioning critical supersaturation" (Nenes and Seinfeld, 2003), that defines the boundary between the CCN populations. In Equation (14), $I_1(0,s_{part})$

represents the growth of CCN for which $D_p^2(\tau) << 2G\int_{\tau}^{t_{\max}} s dt$, or those that experience significant growth beyond the point where they are exposed to $s > s_c$. $I_2(s_{part},s_{max})$ expresses the growth of CCN that do not strictly activate, or do not experience significant growth beyond their critical diameter for which we assume $D_p^2(\tau) >> 2G\int_{\tau}^{t_{\max}} s dt$. With these simplifications, $I_1(0, s_{part})$ and $I_2(s_{part}, s_{max})$ (using Equation 8) become,

$$I_1(0, s_{part}) = \int_0^{S_{part}} \left(\frac{G}{aV}\right)^{1/2} \left(s_{\max}^2 - s^2\right)^{1/2} \frac{2N_i}{3s\sqrt{2\pi}\ln\sigma_i} \exp\left\{\frac{-\ln^2\left[\left(s_{g,i}/s\right)^{2/3}\right]}{2\ln^2\sigma_i}\right\} ds \quad (15)$$

$$I_2(s_{part}, s_{\max}) = \int_{S_{part}}^{S_{\max}} \frac{2A}{3s} \frac{2N_i}{3s\sqrt{2\pi}\ln\sigma_i} \exp\left\{\frac{-\ln^2\left[\left(s_{g,i}/s\right)^{2/3}\right]}{2\ln^2\sigma_i}\right\} ds \quad (16)$$

where $s_{g,i}$ is given by

$$s_{g,i} = \sqrt{\frac{4A^3\rho_w M_s}{27\nu\rho_s M_w D_{p,g}^3}} \quad (17)$$

M_s is the solute molecular weight, ν is the effective Van't Hoff factor and ρ_s is the density of the solute and $A=4M_w\sigma/RT\rho_w$. Equation (17) assumes that the CCN are completely soluble; appropriate modifications should be used if the CCN contain a slightly soluble (Laaksonen *et al*., 1998), insoluble (e.g., Seinfeld and Pandis, 1998) or surfactant fraction (Rissman *et al*., 2004).

The integration of Equations (15) and (16) can be done with the help of the transformation coefficient $u = \frac{\ln\left(s_{g,i}/s\right)^2}{3\sqrt{2}\ln\sigma_i}$, and by approximating $\left(1 - \frac{s_{g,i}}{s_{\max}}\right)^{1/2}$ in Equation (15) with $1 - \frac{1}{2}\frac{s_{g,i}}{s_{\max}}$,

$$I_1(0, s_{part}) = \frac{N_i}{2}\left(\frac{G}{aV}\right)^{1/2} s_{\max}\left\{erfc\left(u_{part}\right) - \frac{1}{2}\left(\frac{s_{g,i}}{s_{\max}}\right)^2 \exp\left(\frac{9\ln^2\sigma_i}{2}\right)\cdot erfc\left(u_{part} + \frac{3\ln\sigma_i}{\sqrt{2}}\right)\right\} \quad (18)$$

$$I_2(s_{part}, s_{\max}) = \frac{AN_i}{3s_{g,i}} \exp\left(\frac{9\ln^2\sigma_i}{8}\right)\left[erf\left(u_{part} - \frac{3\ln\sigma_i}{2\sqrt{2}}\right) - erf\left(u_{\max} - \frac{3\ln\sigma_i}{2\sqrt{2}}\right)\right] \quad (19)$$

where

$$u_{part} = \frac{\ln\left(s_{g,i}/s_{part}\right)^2}{3\sqrt{2}\ln\sigma_i}\ , \quad u_{\max} = \frac{\ln\left(s_{g,i}/s_{\max}\right)^2}{3\sqrt{2}\ln\sigma_i} \quad (20)$$

It should be noted that the integrals in equations (18) through (20) bears some similarity with the formulations of Abdul-Razzak et al. (1998); this similarity arises from the usage of lognormal distributions. However, our formulations are distinctly different, as, *i*) they arise from the application of population splitting and thus use the integrals in a distinct manner, and, *ii*) lack the post-integration modifications applied by Abdul-Razzak et al. (1998).

2.5 Using the parameterization

The procedure for using the modal formulation is similar to the sectional aerosol formulation (Nenes and Seinfeld, 2003). Figure 1 displays the solution algorithm for the lognormal aerosol formulation. s_{part} is calculated using the "descriminant criterion", or the sign of the quantity $\Delta = \left(s_{\max}^4 - \frac{16A^2\alpha V}{9G}\right)$. Δ expresses the extent of kinetic limitations throughout the droplet population; $\Delta = 0$ marks a boundary between two droplet growth regimes, one where most CCN are free from kinetic limitations $(\Delta > 0)$

and one in which kinetic limitations are dominant $(\Delta < 0)$. When $\Delta > 0$, s_{part} is given by an analytical expression as $s_{part} = s_{\max}\left\{\frac{1}{2}\left[1+\left(1-\frac{16A^2aV}{9Gs_{\max}^4}\right)^{1/2}\right]\right\}^{1/2}$; when $\Delta < 0$, s_{part} is determined by an empirical correlation, $s_{part} = s_{\max}\min\left\{\frac{2\cdot 10^7 A}{3}s_{\max}^{-0.3824}, 1.0\right\}$. After determining s_{part}, Equations (18) and (19) are substituted into Equation (10), and solved for s_{max} using the bisection method. The number of droplets is computed from Equation (9). An evaluation of the modal formulation is provided in section 5.

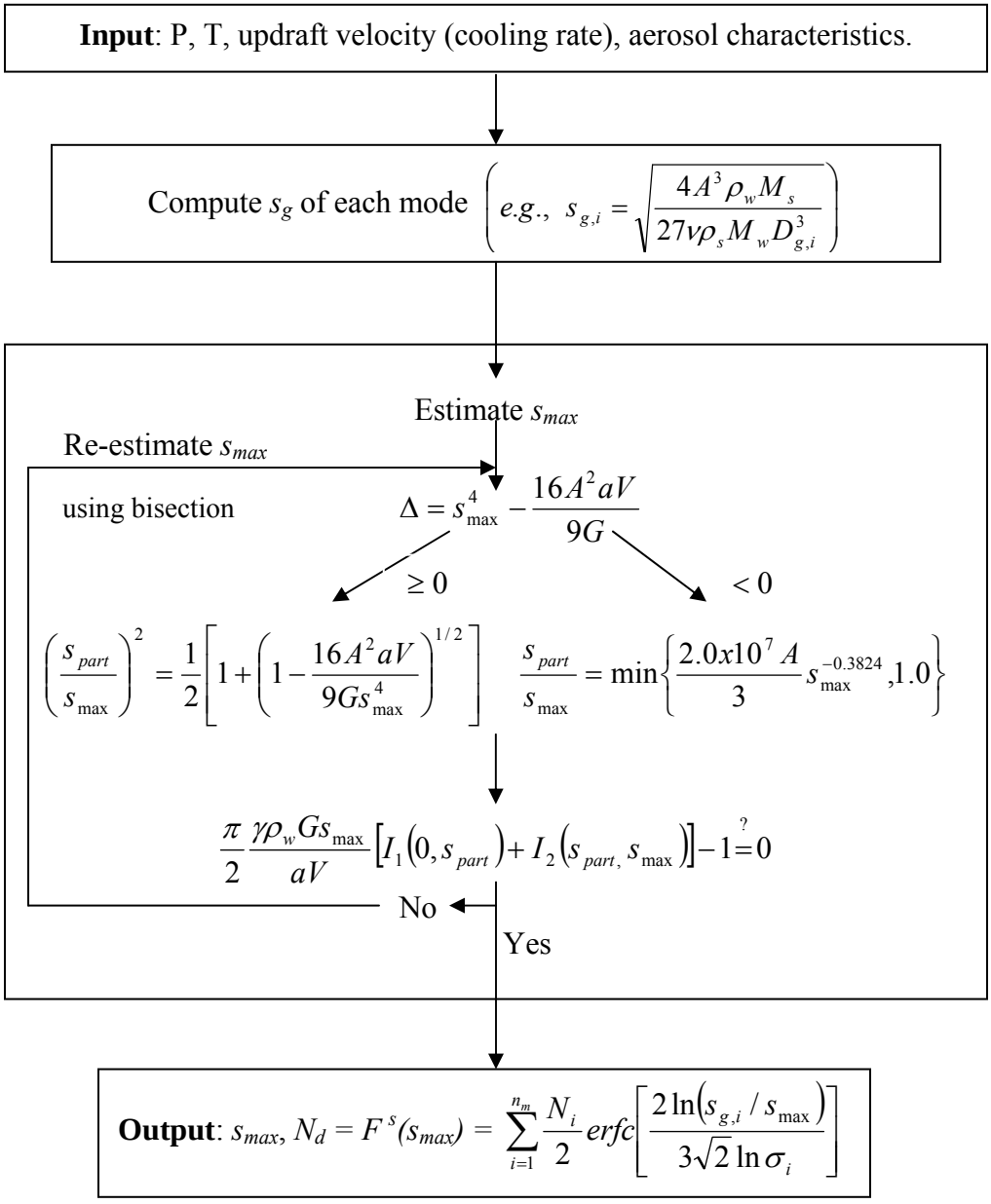

Figure 1 Parameterization algorithm (lognormal formulation)

CHAPTER 3

INCLUDING SIZE – DEPENDANT GROWTH KINETICS INTO NS

3.1 Introduction

In developing the sectional and modal formulations of NS, we have assumed that the diffusivity of water vapor onto the droplets, $D_v^{'}$, is independent of their size. Although a good approximation for water droplets larger than 10μm (Seinfeld and Pandis, 1998), it substantially decreases for smaller and potentially multicomponent drops (Seinfeld and Pandis, 1998). As a result, water vapor condensation in the initial stages of cloud formation is overestimated and the stronger competition for water vapor biases the parcel supersaturation towards lower values. This results in an underestimation of cloud droplet concentration, which worsens if the presence of film-forming compounds further impedes the growth rate. It is important to note that other mechanistic parameterizations (e.g., Ghan *et al*., 1993; Abdul-Razzak *et al*., 1998; Rissman *et al*., 2004) also neglect size-dependence of the diffusivity coefficient and also tend to underestimate N_d (Nenes and Seinfeld, 2003).

Size effects on water vapor diffusivity can be introduced by the following relationship (Fukuta and Walter, 1970),

$$D_v^{'} = \frac{D_v}{1 + \frac{2D_v}{a_c D_p}\sqrt{\frac{2\pi M_w}{RT}}} \tag{21}$$

where a_c is the accommodation coefficient, a fundamental parameter that expresses the probability of a water vapor molecule remaining in the droplet phase upon collision (Seinfeld and Pandis, 1998),

$$a_c = \frac{\text{number of molecules entering the liquid phase}}{\text{number of molecular collisions with the droplet surface}}$$

For pure water, a_c ranges between 0.1 and 0.3 (Li *et al.,* 2001) but an aged atmospheric droplet tends to have a lower accommodation coefficient, typically between 0.04 and 0.06 (Pruppacher and Klett, 2000; Shaw and Lamb, 1999; Conant et al., 2004). The presence of organic films can further decrease the accommodation coefficient; although still controversial, there are indications that such compounds exist in the atmosphere (e.g., Chuang, 2003).

For typical droplet sizes, D_v' depends strongly on a_c (Equation 21). For a value of a_c close to unity, the difference between D_v' and D_v is less than 25% for particles larger than 1 μm and less than 5% for droplet diameters larger than 5μm. However, D_v' becomes significantly lower than D_v if $a_c<1$ (Seinfeld and Pandis, 1998). Therefore, introducing the dependence of D_v' on size and a_c is important to eliminate biases in droplet activation. The thermal conductivity of air, k_a' (Equation 12), also has a dependence on size, which is rather weak for the droplet sizes of interest. Simulations (not shown here) confirm that introducing a size-dependant thermal conductivity is not necessary.

3.2 Implementing size-dependant D_v into NS

Equation (21) could be substituted into Equation (12) in order to account for the size-dependence on D_v'. However, in such a case, Equation (13) becomes impractical in its implementation. An alternate approach is needed.

Two approaches can be used to introduce corrections to D_v: i) using an average value for the diffusivity, $D_{v,ave}$, for those CCN that activate, and, ii) calculating D_v' for each CCN section. We choose to adopt the first approach because it can be used in both sectional and modal formulations of the NS parameterization (while the second approach cannot), and, the second approach adds upon the computational burden. A section-specific D_v method has also been developed (Ming *et al.*,*JAS*, in press). For simplicity, we adopt a size-averaged diffusion coefficient, $D_{v,ave}$,

$$D_{v,ave} = \frac{\int_{D_{p,low}}^{D_{p,big}} D_v' dD_p}{\int_{D_{p,low}}^{D_{p,big}} dD_p} \tag{22}$$

where $D_{p,big}$ and $D_{p,low}$ are the upper and lower size bounds used for calculating the average. Substituting Equation (21) into (22) and integrating yields:

$$D_{v,ave} = \frac{D_v}{D_{p,big} - D_{p,low}} \left[\left(D_{p,big} - D_{p,low} \right) - B \cdot \ln\left(\frac{D_{p,big} + B}{D_{p,low} + B} \right) \right] \tag{23}$$

where $B = \frac{2D_v}{a_c} \cdot \left(\frac{2\pi M_w}{RT} \right)^{1/2}$. In deriving Equation (23), we assume that a_c remains constant throughout the activation process.

If $D_{p,big}$ and $D_{p,low}$ and a_c are known, Equation (23) can be used to calculate $D_{v,ave}$, and substituted into the G term (Equation 13) of NS. a_c is usually constrained from

observations (e.g., Chuang *et al.,* 2003; Conant *et al.*, 2004). What remains is the determination of the $D_{p,big}$ and $D_{p,low}$.

3.3 Determination of $D_{p,big}$ and $D_{p,low}$

We have evaluated two methods for calculating $D_{p,big}$ and $D_{p,low}$:

Empirical determination of $D_{p,big}$ and $D_{p,low}$.

A set of numerical parcel model simulations were used to determine $D_{p,big}$ and $D_{p,low}$ that, after substitution into Equation (23) (and subsequently into NS), would give a parameterized N_d in agreement with the numerical parcel predictions. Published literature suggests values for a_c as low as 10^{-5} (e.g., Chuang, 2003) during the initial stages of particle growth; if true, such CCN would experience a "slow growth" phase (with a very low a_c) followed by a "fast growth" phase with much higher a_c. Simulations with the Nenes *et al.* (1998) parcel model suggests that CCN with a constant $a_c \sim 10^{-3}$ experiences roughly the same growth as a "film-breaking" CCN with a slow-growth phase $a_c \sim 10^{-5}$ and a rapid-growth phase $a_c \sim 0.042$. Therefore, a_c is assumed to vary between 0.001 and 1.0.

$D_{p,big}$ and $D_{p,low}$ were determined for the wide set of conditions and a_c listed in Table 1. Optimization criteria were the minimization of error and standard deviation between parameterized and parcel model N_d. Tables 2, 3 and 4, shown in the Appendix, represent a small sample of the simulations done during the optimization process.

Table 1 Simulations considered for empirically determining $D_{p,big}$ and $D_{p,low}$ of $D_{v,ave}$

Property	**Value / Range**
Cloud height (m)	500
N_i (cm^{-3})	100, 500, 1000, 5000, 10000
σ_i	1.1, 1.2, 1.5, 1.5, 2.0, 2.5
$D_{p,g}$ (μm)	0.025, 0.05, 0.75, 0.5, 0.25
V (ms^{-1})	0.1, 0.3, 1.0, 3.0
Chemical composition	$(NH_4)_2SO_4$:100%, $(NH_4)_2SO_4$:50% - insoluble:50%, NaCl:100%, NaCl:25% - insoluble:75%
Accommodation coefficient	0.001, 0.005, 0.042, 0.01, 0.1, 1.0
Pressure (mbar)	100, 500, 800, 1000
Relative humidity	90%, 98%
Temperature (K)	273, 293, 303, 310

The first two columns of these tables show the values of $D_{p,big}$ and $D_{p,low}$ considered in the simulations whereas the last two columns depict the average error and standard deviation derived from the comparison of parameterized and parcel model N_d. The optimum $D_{p,big}$ was found to be 5 μm, while the optimum $D_{p,low}$ was found to vary with a_c; a correlation that relates the optimum $D_{p,low}$ and a_c was then derived,

$$D_{p,low} = \min\left\{0.207683 \cdot a_c^{-0.33048}, 5.0\right\} \tag{24}$$

where $D_{p,low}$ is given in μm.

From Equation (24), a_c increases with decreasing $D_{p,low}$. This is expected; for large a_c, small CCN experience less kinetic limitations, and therefore can activate into droplets (Nenes *et al.*, 2001). As a result, a wider range of CCN sizes need to be considered in the calculation of $D_{v,ave}$, so $D_{p,low}$ should decrease. When a_c decreases, only the largest of CCN (with low s_c) have enough time to activate; hence a narrow range of CCN sizes can contribute to droplet number concentration, thus increasing $D_{p,low}$.

Theoretical determination of $D_{p,big}$ and $D_{p,low}$.

$D_{p,big}$ and $D_{p,low}$ may also be determined using theoretical arguments. One can be derived from the equation that describes the diffusional growth of a droplet from time τ (when the parcel supersaturation is equal to the CCN critical supersaturation, s_c), to the time of maximum supersaturation, t_{max} (Nenes and Seinfeld, 2003),

$$D_p^2 = D_p^2(\tau) + 2\int_{\tau}^{t_{\max}} G\, s\, dt \tag{25}$$

$D_p(\tau)$, like in Equation (13), is assumed to be equal to the critical diameter $D_c=8M_w\sigma/3RT\rho_w s_c$, while the supersaturation integral in Equation (25) can be evaluated using the lower bound of Twomey (1959):

$$\int_{\tau}^{t_{\max}} s\,dt \approx \frac{1}{2aV}[s_{\max}^2 - s(\tau)^2] \tag{26}$$

where $s(\tau)$ is the parcel supersaturation at time τ. Substituting Equation (26) into (25), we eventually obtain

$$D_p = \sqrt{\left(\frac{2A}{3s_{c,\min}}\right)^2 + \frac{G}{aV}\left[s_{\max}^2 - s_{c,\min}^2\right]}, \tag{27}$$

where $s_{c,min}$ is the critical supersaturation of the largest CCN that exceeds its critical diameter. Equation (27) can be used as an estimate for the upper limit $D_{p,big}$. The lower limit, $D_{p,low}$, can be estimated by the smallest CCN that can theoretically activate:

$$D_{p,low} = \frac{2A}{3s_{\max}} \tag{28}$$

It is notable that in this method, $D_{p,big}$ depends on a_c as opposed to the empirical method where $D_{p,low}$ depends on a_c.

Assessment of $D_{p,big}$ and $D_{p,low}$ calculation methods

Both methods of calculating $D_{v,ave}$ were introduced into the NS parameterization; N_d predictions were then compared with parcel model simulations. The comparisons were done for the activation of single mode lognormal aerosol with $D_{p,g}$ ranging between 0.025 to 0.25μm, σ_i between 1.1 to 2.5, and for updraft conditions ranging between V = 0.1 to 3.0 ms^{-1}. Ambient P and T were set to 800 mbar and 283 K, respectively. Figure 2 shows

the parameterized droplet number concentration (using the two different methods of estimating $D_{v,ave}$) against the parcel model simulations. The 1:1 line represents a perfect agreement between the parameterization and the parcel model. Results are presented for two values of the accommodation coefficient ($a_c = 0.042$, $a_c = 0.1$). An average error of 6% (±1%) was observed for the theoretical method, which slightly underperforms against the empirical method (average error=2%, ±0.9%). We thus choose to use the empirical method until an alternate theoretical criterion is derived.

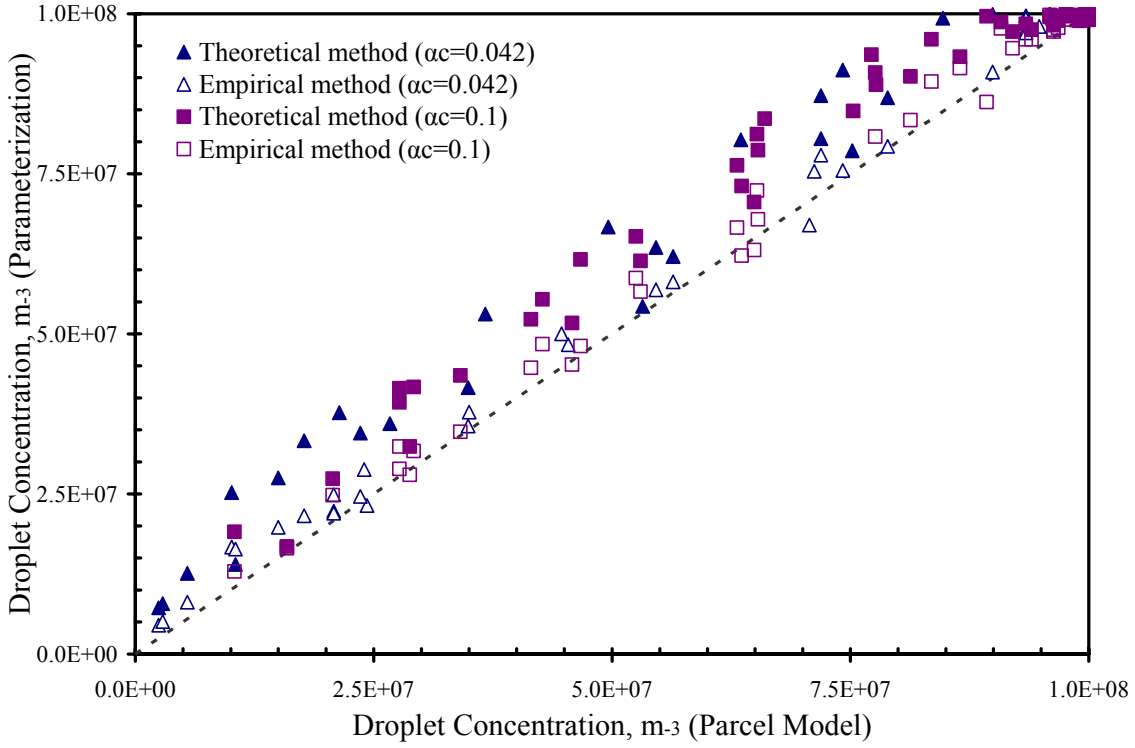

Figure 2 Droplet number concentration as predicted by the modified NS parameterization and by the cloud parcel model, using the sectional formulation. Results for both theoretical and empirical $D_{v,ave}$ are presented. The other simulation characteristics are given in the text

CHAPTER 4

EVALUATION OF MODIFIED NS PARAMETERIZATION

4.1 Method

The sectional formulation of the parameterization, as well as the diffusivity modification were assessed for their ability to reproduce simulations from the adiabatic cloud parcel model of Nenes *et al*., (2001) over a large range of aerosol size distributions and updraft velocities. The detailed numerical parcel model used in this study has been widely used and recently evaluated with in-situ data (Conant *et al*., 2004). Table 5 shows the simulation sets used for the evaluation of the parameterization with updraft velocities ranging from 0.1 – 3.0m/s. Both single and tri-modal aerosols were considered, for number concentrations and mode diameters characteristic of tropospheric aerosol. For trimodal aerosol, we have selected four of the *Whitby* (1978) trimodal representations, namely the marine, clean continental, average background, and urban aerosol representations (Table 6). The updraft velocities used in our evaluation ranges between 0.03 and 3.0 m s^{-1}; together with the wide range of aerosol number concentrations considered, s_{max} varies from 0.01% to over 1%, covering the climatically important range of cloud droplet formation conditions.

Table 5 Aerosol and updraft velocity conditions considered in the parameterization evaluation

Simulation set[b,c]	$D_{g,i}$, **µm**	N_i, **cm^{-3}**	σ_i	W, **ms^{-1}**	**Chemical Composition**	**Number of cases**
SM1	0.025	100	1.1 - 1.5	0.1 - 3.0	$(NH_4)_2SO_4$:100%	15
SM2	0.025	500	1.1 - 1.5	0.1 - 3.0	$(NH_4)_2SO_4$:100%	15
SM3	0.05	500	1.1 - 2.5	0.1 - 3.0	NaCl:100%	25
SM4	0.25	100	1.1 - 2.5	0.1 - 3.0	NaCl:100%	25
SM5	0.75	1000	1.1 - 2.5	0.1 - 3.0	$(NH_4)_2SO_4$:100%	25
TM-M	Given in Table 3				$(NH_4)_2SO_4$:100%	4
TM-C					$(NH_4)_2SO_4$:100%	4
TM-B					$(NH_4)_2SO_4$:100%	4
TM-U					$(NH_4)_2SO_4$:100%	4

[b] SM denotes single mode

[c] TM denotes trimodal; M represents marine, C continental, B background, and U urban aerosol

Table 6 Aerosol characteristics for the multimodal simulations of Table 2. Distributions taken from Whitby (1978). $D_{g,i}$ is in μm; N_i is in cm^{-3}.

Aerosol Type	Nuclei Mode			Accumulation mode			Coarse mode		
	$D_{g,1}$	σ_1	N_1	$D_{g,2}$	σ_2	N_2	$D_{g,3}$	σ_3	N_3
Marine	0.010	1.6	340	0.070	2.0	60	0.62	2.7	3.1
Continental	0.016	1.6	1000	0.068	2.1	800	0.92	2.2	0.72
Background	0.016	1.7	6400	0.076	2.0	2300	1.02	2.16	3.2
Urban	0.014	1.8	106000	0.054	2.16	32000	0.86	2.21	5.4

4.2 Evaluation of the modal formulation

Evaluation of the modal formulation is done by comparing its predictions of N_d with those of the sectional parameterization. We consider the activation of lognormal aerosol, so both formulations should give the same droplet number (provided the discretization error of the sectional formulation is insignificant). This is shown in Figure 3, which depicts the parameterized N_d, using the sectional vs. the modal formulation. Cases considered were for a single mode lognormal aerosol with $D_{p,g}$ ranging between 0.05 to 0.75μm, σ_i ranging between 1.1 to 2.5, and for updraft conditions ranging between V = 0.1 to 3.0 ms^{-1}. The sectional formulation used 200 sections for discretizing the lognormal distribution.

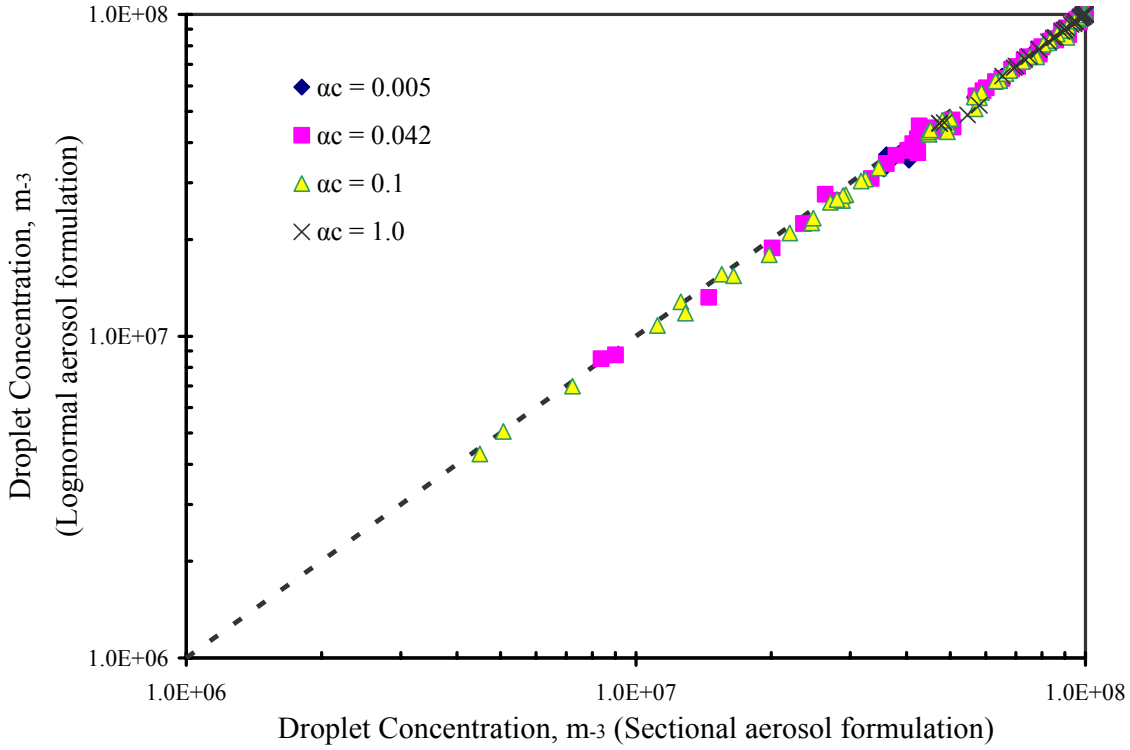

Figure 3 Droplet number concentration as predicted by the modified NS parameterization using the sectional and the modal formulations. Cases considered were for a single mode lognormal aerosol with $D_{p,g}$ ranging between 0.05 to 0.75μm, σ_i ranging between 1.1 to 2.5, updraft conditions ranging between V = 0.1 to 3.0 ms^{-1} and for chemical composition of pure $(NH_4)_2SO_4$, pure NaCl, and 50% $(NH_4)_2SO_4$ - 50% insoluble. Ambient P and T were set to 800 mbar and 283 K, respectively. The sectional formulation used 200 sections for discretizing the lognormal distribution. Results are for four values of a_c

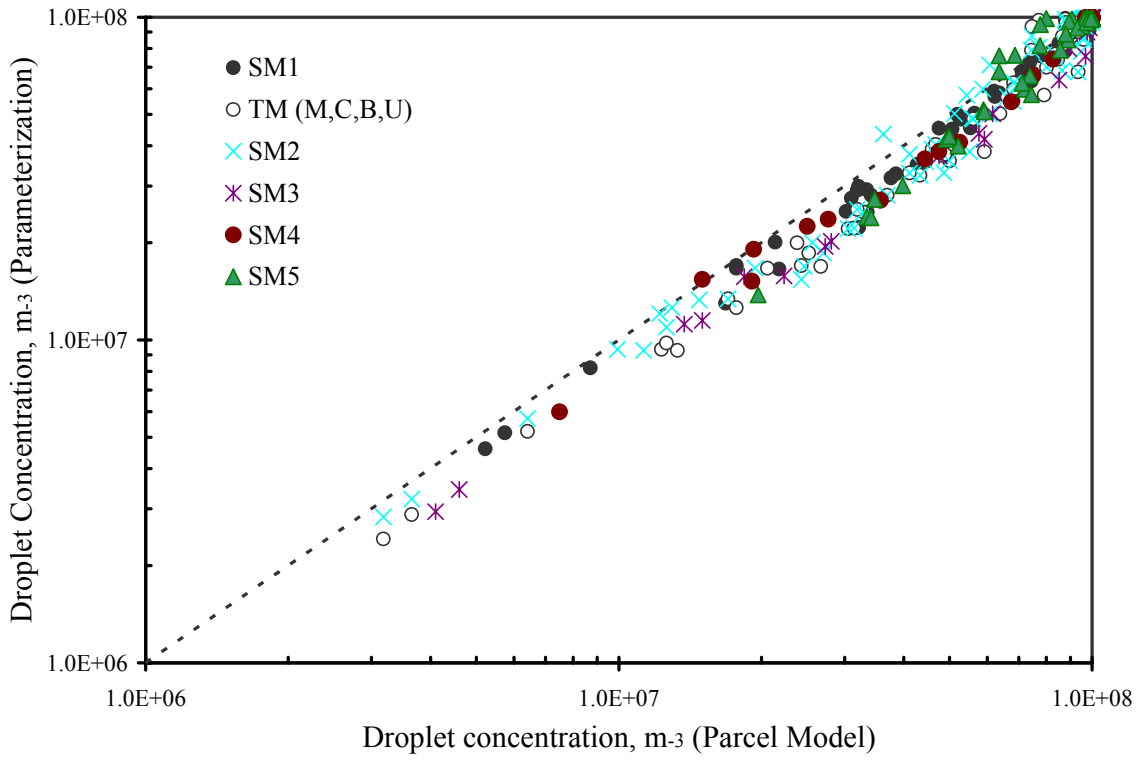

Figure 4 Droplet number concentration as predicted by the NS parameterization and by the cloud parcel model for all the aerosol size distributions and updraft velocities of Table 2. All simulations assume perfect water vapor accommodation ($a_c = 1.0$), P = 800mbar and $T = 283$K

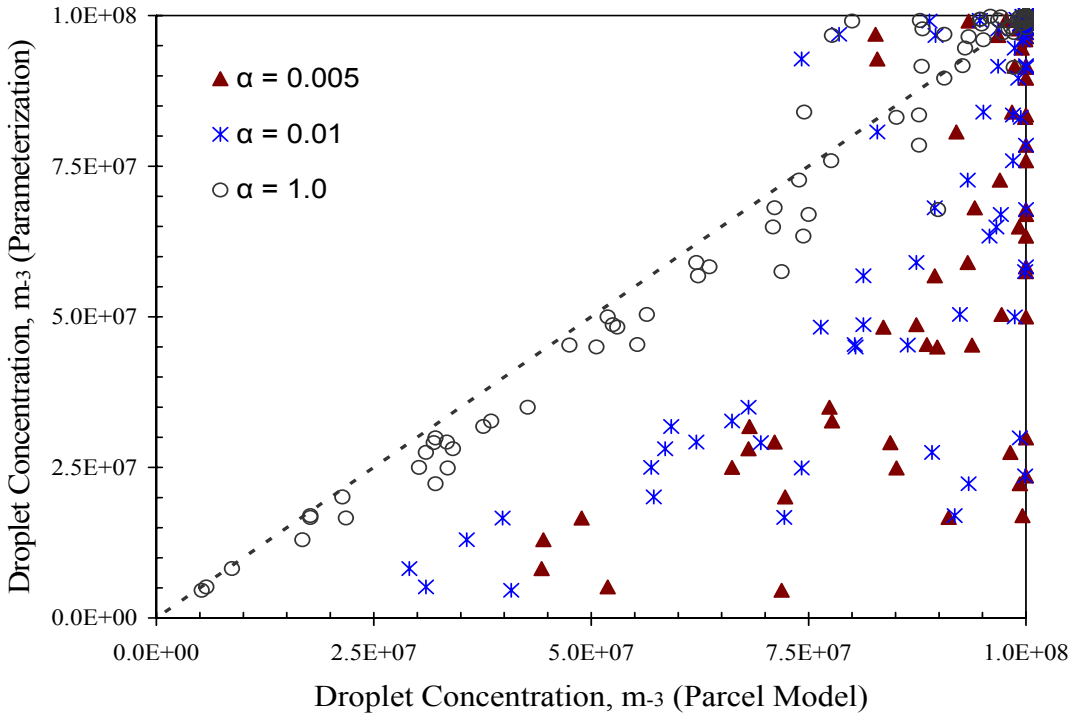

Figure 5 Droplet number concentration as predicted by the NS parameterization and by the cloud parcel model for cases SM1, SM2 and SM3 of Table 2, and for a_c = 1.0, a_c = 0.01, and a_c = 0.005. All simulations assume P = 800mbar and T = 283K

Regardless of activation conditions, the parameterization with modal formulation is as robust as the parameterization with the sectional representation (average error $\approx 1\%$, standard deviation $\approx 0.3\%$). Therefore, for lognormal aerosol, both formulations can be interchanged without any loss in accuracy. The advantage of using the lognormal distribution is that it is simpler to implement and, more than two orders of magnitude faster on a Pentium PC, than the sectional formulation (with 200 sections).

4.3 Evaluation of parameterization with modified water vapor mass transfer

Figure 4 displays the droplet number concentration as predicted by NS and by the (Nenes *et al*., (2001)) parcel model for the aerosol conditions of Table 3. The parameterized droplet number concentrations closely follow the parcel model simulations; however, there is a tendency for underestimation, which is not significant for a_c=1.0, but worsens as a_c decreases (Figure 5). This problem is resolved by substituting D_v' in the G term of Equation (17) with the modified diffusivity, $D_{v,ave}$. Figures 6 and 7 display the droplet number concentration from the modified parameterization against the parcel model predictions for the single mode (Figure 6) and trimodal (Figure 7) aerosol of Table 2. Results are presented for a_c = 0.042 and a_c = 0.005. In Figure 8 we evaluate the parameterization for the simulation conditions considered in Table 7. Results are presented for a_c=0.95, for updraft velocities ranging from 0.03 – 10m/s and for pure ammonium sulfate. It is clear that the modified parameterization captures the parcel model simulations much better than the original NS, even for low values of a_c. The overestimation (average error 4.1±1.3%) observed in Figure 7 for marine aerosol is

caused by the fact that the descriminant for these aerosol is close to zero, at the transition between the kinetically limited ($\Delta>0$) and kinetically free ($\Delta<0$) regimes. Under such conditions, the expression for calculating s_{part} is least accurate. Nevertheless, the modified diffusivity remarkably improves the performance of the parameterization, even for such challenging aerosol as those with film forming compounds. It should also be noted that the modifications pose negligible computational burden, as opposed to employing a more expensive algorithm (e.g., a section-specific D_v').

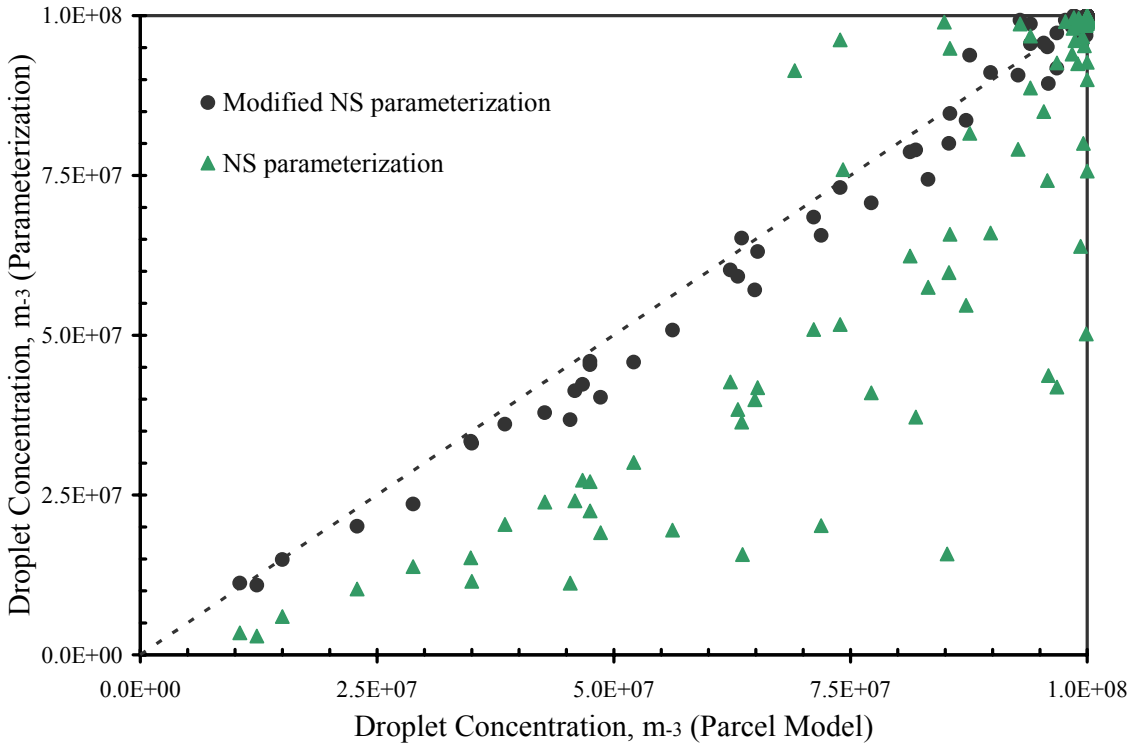

Figure 6 Droplet number concentration as predicted by the modified NS parameterization and by the cloud parcel model for cases SM3 and SM4 of Table 5, and for a_c = 0.042. All simulations assume P = 800mbar and T = 283K

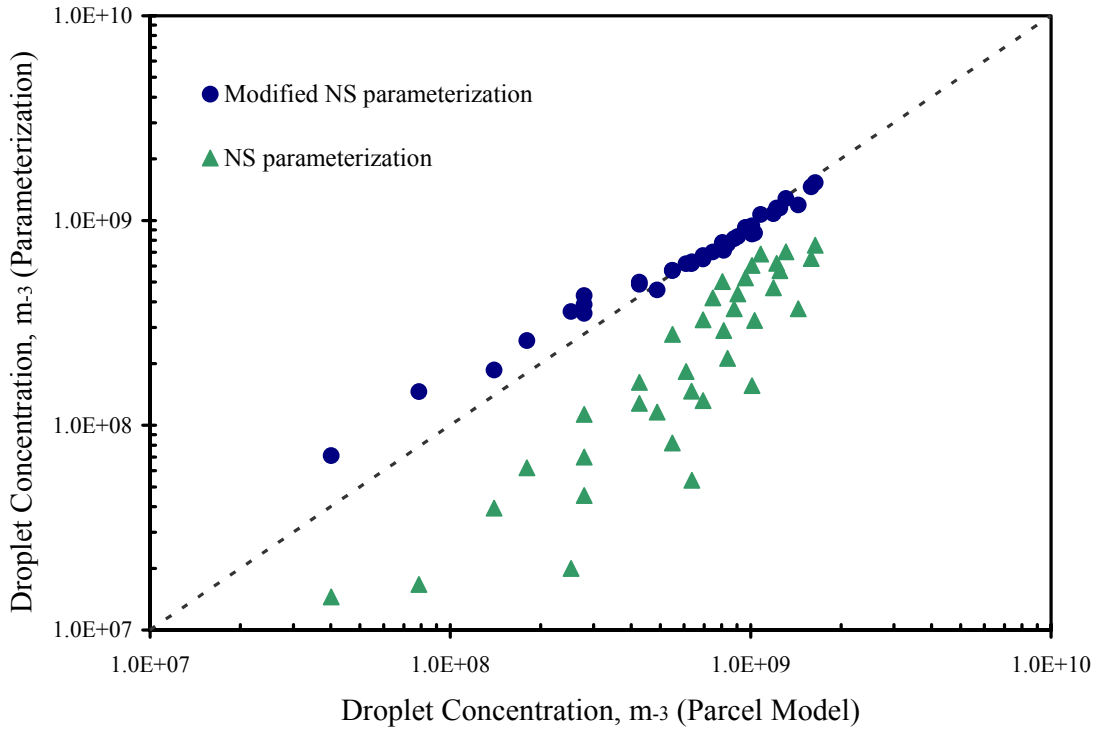

Figure 7 Droplet number concentration as predicted by the modified NS parameterization and by the cloud parcel model for case TM of Table 5, and for $a_c = 0.005$. All simulations assume P = 800mbar and T = 283K

CHAPTER 5

CONCLUSIONS

The aerosol activation parameterization developed by Nenes and Seinfeld (2003) was extended to *i)* allow for a lognormal representation of aerosol size distribution, and, *ii)* include a size-dependant mass transfer coefficient for the growth of water droplets (which explicitly includes the accommodation coefficient). To address this, an average value of the water vapor diffusivity is introduced in the parameterization. Two methods were explored for determining the upper and lower bound of the droplet diameter needed for calculating the average water vapor diffusivity. The most accurate employs an empirical correlation derived from numerical parcel simulation.

Predictions of the modified NS parameterization are compared against detailed cloud parcel activation model simulations for a wide variety of aerosol activation conditions. The modified NS parameterization closely tracks the parcel model simulations, even for low values of the accommodation coefficient, without any increase in computational cost. It displays superior performance in both accuracy and robustness. The structure of the parameterization allows for further extension such as the inclusion of entrainment in the parcel (nonadiabatic activation), the use of variable updraft velocities and the treatment of precipitation formation.

The modified NS parameterization was tested not only with a detailed adiabatic cloud parcel model, but with in-situ data as well. Meskhidze *et al.*, (*J.Geoph.Res.,* in press)

evaluated the accuracy of the present work by comparing its results against extensive microphysical data for cumuliform and stratiform clouds of marine and continental origin. In-situ data sets of aerosol size distribution, chemical composition, and updraft velocities were used as input for the modified NS parameterization, and the evaluation was carried out by comparing predicted cloud droplet number concentrations with observations. It was found that, on average, predicted droplet number concentration in adiabatic regions was within ~20% of observations at the base of cumuliform clouds and ~30% of observations at different altitudes throughout the stratiform clouds, all within experimental uncertainty.

This work offers a much needed rigorous and computationally inexpensive framework for directly linking complex chemical effects on aerosol activation in global climate models. Although much is still unknown about the collision-coalescence process, the ability to parameterize this process for calculating changes in precipitation from the increased aerosol loadings is highly desirable, as it establishes the framework for a comprehensive assessment of the aerosol indirect effect.

Table 7 Size distribution parameters of single mode (SM) and tri-modal (TM) test cases shown in figure 8

	Mode 1			**Mode 2**			**Mode 3**		
Test case	N_1	$D_{g,1}$	σ_1	N_2	$D_{g,2}$	σ_2	N_3	$D_{g,3}$	σ_3
SM1	200	0.02	2.5						
SM2	1000	0.02	2.5						
SM3	1000	0.02	1.5						
SM4	200	0.2	2.5						
SM5	10000	0.02	2.5						
TM1-M	340	0.01	1.6	60	0.07	2.0	3.1	0.62	2.7
TM2-M	680	0.01	1.6	120	0.07	2.0	6.2	0.62	2.7
TM1-C	1000	0.016	1.6	800	0.068	2.1	0.72	0.92	2.2
TM2-C	2000	0.016	1.6	1600	0.068	2.1	1.44	0.92	2.2
TM1-B	6400	0.016	1.7	2300	0.076	2.0	3.2	1.02	2.16
TM2-B	12800	0.016	1.7	4600	0.076	2.0	6.4	1.02	2.16
TM1-U	106000	0.014	1.8	32000	0.054	2.16	5.4	0.86	2.21
TM2-U	212000	0.014	1.8	64000	0.054	2.16	10.8	0.86	2.21

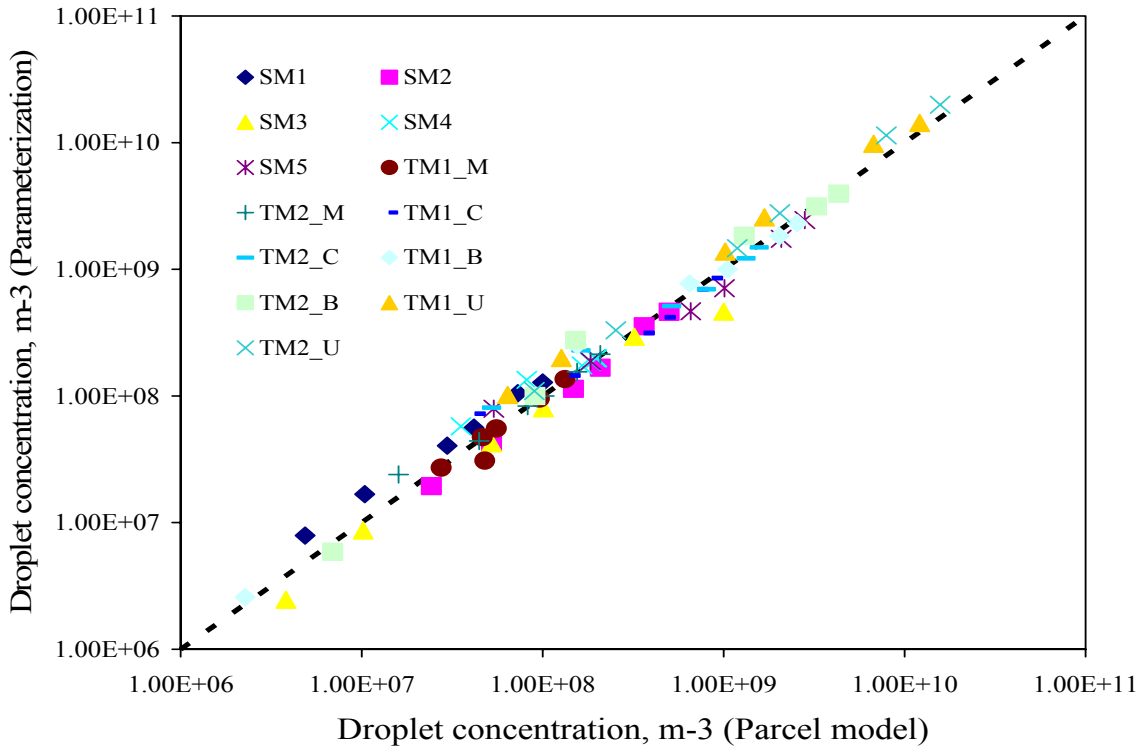

Figure 8 Droplet number concentration as predicted by the modified NS parameterization and by the cloud parcel model for all cases considered in Table 7. All simulations assume P = 800mbar and T = 283K

APPENDIX A

SIMULATIONS USED FOR DERIVING THE OPTIMAL $D_{p,low}$, $D_{p,big}$ USED FOR CALCULATING $D_{V,AVE}$

Table 2 Simulation data for the optimization process of $D_{p,big}$ and $D_{p,low}$ (α_c=0.001)

$D_{p,big}$ (μm)	$D_{p,low}$ (μm)	Avg. error (%)	Std. dev. (%)
5	0.05	0.82	3.0
5	0.5	0.66	2.57
5	1.0	0.49	2.14
5	1.5	0.32	1.77
5	2.0	0.16	1.49
5	2.5	0.007	1.31
5	3.0	0.17	1.29
5	3.5	0.33	1.42
5	4.0	0.49	1.65
5	4.5	0.64	1.93
10	0.05	0.8	2.25
10	0.5	0.93	2.54
10	1.0	1.1	2.87
10	1.5	1.22	3.21
10	2.0	1.36	3.54
10	2.5	1.49	3.88
10	3.0	1.63	4.19
10	3.5	1.76	4.50
10	4.0	1.89	4.80
10	4.5	2.01	5.09
20	0.05	3.23	7.76
20	0.5	3.32	7.96
20	1.0	3.42	8.17
20	1.5	3.52	8.37
20	2.0	3.62	8.57
20	2.5	3.71	8.75
20	3.0	3.81	8.95
20	3.5	3.91	9.13
20	4.0	4.0	9.31
20	4.5	4.1	9.49

Table 3 Simulation data for the optimization process of $D_{p,big}$ and $D_{p,low}$ (α_c=0.005)

$D_{p,big}$ (μm)	$D_{p,low}$ (μm)	Avg. error (%)	Std. dev. (%)
5	0.05	1.46	4.63
5	0.5	1.07	4.02
5	1.0	0.65	3.61
5	1.5	0.26	3.5
5	2.0	0.27	3.63
5	2.5	-0.44	3.92
5	3.0	-0.77	4.32
5	3.5	-1.1	4.75
5	4.0	-1.38	5.21
5	4.5	-1.66	5.67
10	0.05	-1.85	5.99
10	0.5	-2.1	6.41
10	1.0	-2.37	6.86
10	1.5	-2.62	7.29
10	2.0	-2.87	7.71
10	2.5	-3.1	8.1
10	3.0	-3.33	8.49
10	3.5	-3.55	8.85
10	4.0	-3.76	9.25
10	4.5	-3.96	9.54
20	0.05	-5.63	12.2
20	0.5	-5.78	12.4
20	1.0	-5.93	12.7
20	1.5	-6.08	12.9
20	2.0	-6.23	13.1
20	2.5	-6.37	13.4
20	3.0	-6.51	13.6
20	3.5	-6.64	13.8
20	4.0	-6.77	14.0
20	4.5	-6.9	14.1

Table 4 Simulation data for the optimization process of $D_{p,big}$ and $D_{p,low}$ (α_c=0.042)

$D_{p,big}$ (μm)	$D_{p,low}$ (μm)	Avg. error (%)	Std. dev. (%)
5	0.05	2.90	9.4
5	0.5	1.96	8.78
5	1.0	0.08	8.1
5	1.5	0.33	8.4
5	2.0	-0.31	8.6
5	2.5	-0.87	8.9
5	3.0	-1.37	9.1
5	3.5	-1.81	9.2
5	4.0	-2.2	9.65
5	4.5	-2.55	9.78
10	0.05	-2.12	9.81
10	0.5	-2.52	9.98
10	1.0	-2.92	10.1
10	1.5	-3.28	10.32
10	2.0	-3.60	10.45
10	2.5	-3.88	10.56
10	3.0	-4.14	10.76
10	3.5	-4.38	10.99
10	4.0	-4.60	11.45
10	4.5	-4.8	11.39
20	0.05	-5.45	11.69
20	0.5	-5.63	11.9
20	1.0	-5.81	12.21
20	1.5	-5.97	12.29
20	2.0	-6.11	12.43
20	2.5	-6.25	12.5
20	3.0	-6.38	12.5
20	3.5	-6.49	12.56
20	4.0	-6.6	12.78
20	4.5	-6.71	12.9

REFERENCES

Abdul-Razzak, H., and S. J. Ghan, A parameterization of aerosol activation: 2. Multiple aerosol types, *J. Geophys. Res*., 105, 6837–6844, 2000.

Abdul-Razzak, H., S. J. Ghan, and C. Rivera-Carpio, A parameterization of aerosol activation. 1. Single aerosol type, *J. Geophys. Res.,* 103 (D6), 6123-6131, 1998.

Boucher, O., and U. Lohmann, The sulfate-CCN-cloud albedo effect-A sensitivity study with 2 general-circulation models, *Tellus, Ser. B*, 47, 281-300, 1995.

Charlson, R. J., J. H. Seinfeld, A. Nenes, M. Kulmala, A. Laaksonen, and M. C. Facchini, Reshaping the theory of cloud formation, *Science*, *292*, 2025-2026, 2001.

Chuang, P.Y., Measurement of the timescale of hygroscopic growth for atmospheric aerosols. *J. Geophys. Res*., *108* (D9), 4282, doi: 10.1029/2002JD002757, 2003.

Chuang, P., R. Charlson, and J. Seinfeld, Kinetic limitation on droplet formation in clouds, *Nature, 390,* 594-596, 1997.

Conant, W. C., Vanreken, T., Rissman, T., Varutbangkul, V., Jimenez, J., Delia, A., Bahreini, R., Roberts, G., Nenes, A., Jonsson, H., Flagan, R.C., Seinfeld, J.H., Aerosol-cloud drop concentration closure in warm cumulus, *J. Geophys. Res*., *109,* D13204, doi:10.1029/2003JD004324, 2004.

Facchini, M.C., M. Mircea, S. Fuzzi, and R. Charlson, Cloud albedo enhancement by surface active organic solutes in growing droplets, *Nature*, *401*, 257-259, 1999.

Feingold, G., and P. Chuang, Analysis of the influence of film-forming compounds on droplet growth: Implications for cloud microphysical processes and climate, *J. Atmos. Sci., 59*, 2006-2018, 2002.

Fukuta, N., and L. A. Walter, Kinetics of hydrometer growth from the vapor; spherical model, *J. Atmos. Sci., 27,* 1160-1172, 1970.

Ghan, S., C. Chuang, and J. Penner, A parameterization of cloud droplet nucleation. part I: Single aerosol species. *Atmos. Res.*, 30, 197-222, 1993.

Ghan, S., L. Leung, R. Easter, and H. Abdul-Razzak, Prediction of cloud droplet number in a general circulation model, *J. Geophys. Res., 102,* 21, 777-21, 794, 1997.

Gultepe, I., and G. Isaac, The relationship between cloud droplet and aerosol number concentrations for climate models, *Int. J. Climatol., 16,* 941 – 946, 1996.

Intergovernmental Panel on Climate Change: *The scientific Basis,* Cambridge Univ. Press, New York, 2001.

Laaksonen, A., P. Korhonen, M. Kulmala, and R. Charlson, Modification of the Köhler equation to include soluble trace gases and slightly soluble substances, *J. Aerosol Sci.*, *155*, 853–862, 1998.

Lance, S., A. Nenes, and T. Rissman, Chemical and dynamical effects on cloud droplet number: Implications for estimates of the aerosol indirect effect. *J. Geoph. Res.,* 109, D22208, doi:10.1029/2004JD004596, 2004.

Li, Z., A. L. Williams, and M. J. Rood, Influence of soluble surfactant properties on the activation of aerosol particles containing inorganic solute, *J. Atm. Sci*., 55, 1859–1866, 1998.

Li, Y. Q., P. Davidovits, Q.Shi, J. T. Jayne, and D. R. Warsnop*,* Mass and thermal accommodation coefficients of $H_2O_{(g)}$ on liquid water as a function of temperature, *J. Phys. Chem. A*, *Vol. 105,* 10627-10634, 2001.

Lohmann, U., J. Feichter, C. C. Chuang and J. E. Penner, Predicting the number of cloud droplets in the ECHAM GCM, *J. Geophys. Res.* 104*,* 9169-9198 and 24,557-24,563 (Erratum), 1999.

Medina, J., and A. Nenes, Effects of film forming compounds on the growth of giant CCN: Implications for cloud microphysics and the aerosol indirect effect, *J. Geophys. Res.*, 109, D20207, doi: 10.1029/2004JD004666, 2004.

Meskhidze, N., A. Nenes, Conant, W. C., and Seinfeld, J.H. Evaluation of a new Cloud Droplet Activation Parameterization with In Situ Data from CRYSTAL-FACE and CSTRIPE, (*J.Geoph.Res.,* in press).

Ming, Y. *et al*., A robust parameterization of cloud droplet activation, (*J.Atmos.Sci.*, in press).

Nenes, A., and J.H. Seinfeld, Parameterization of cloud droplet formation in global climate models, *J. Geophys. Res., 108*(D14) 4415, doi: 10.1029/2002JD002911, 2003.

Nenes, A., R.J. Charlson, M.C. Facchini, M. Kulmala, A. Laaksonen, and J.H. Seinfeld, Can chemical effects on cloud droplet number rival the first indirect effect?, *Geophys. Res. Lett*, 24 (17), 1848, doi: 10.1029/2002GL015295, 2002.

Nenes, A., S. J. Ghan, H. Abdul-Razzak, P. Chuang, and J. Seinfeld, Kinetic limitations on cloud droplet formation and impact on cloud albedo, *Tellus Ser. B,* 53, 133 – 149, 2001.

Pruppacher, H.R. and J.D. Klett, *Microphysics of Clouds and Precipitation*. Kluwer Academic Publishers, Dordrecht, Netherlands, 2000.

Rissman, T., A. Nenes, and J.H. Seinfeld, Chemical amplification (or dampening) of the Twomey effect: Conditions derived from droplet activation theory, *J. Atmos. Sci*., 61(8), 919-930, 2004.

Seinfeld, J.H., and S.N. Pandis, *Atmospheric Chemistry and Physics: From Air Pollution to Climate Change*, John Wiley & Sons, Inc., 1998.

Shantz, N. C., W. R. Leaitch, and P. Caffrey, Effect of organics of low solubility on the growth rate of cloud droplets, *J. Geophys. Res., 108*, doi:10.1029/2002JD002540, 2003.

Shaw R.A. and D. Lamb, Experimental determination of the thermal accommodation and condensation coefficients of water, *J. Chem. Phys*., *111* (23), 1999.

Shulman, M. L., M. C. Jacobson, R. J. Charlson, R. E. Synovec, and T. E. Young, Dissolution behavior and surface tension effects of organic compounds in nucleating cloud droplets, *Geophys. Res. Lett., 23*, 277 – 280, 1996.

Twomey, S., The nuclei of natural cloud formation. II. The supersaturation in natural clouds and the variation of cloud droplet concentration, *Geofisica Pura Appl*., 43, 243-249, 1959.

Whitby, K., The physical characteristics of sulfur aerosols, *Atmos. Environ., 12,* 135-159, 1978.